

Astrophysical S factor for the $^{15}\text{N}(p,\gamma)^{16}\text{O}$ reactionA. M. Mukhamedzhanov,¹ M. La Cognata,² and V. Kroha³¹*Cyclotron Institute, Texas A&M University, College Station, Texas 77843, USA*²*Università di Catania and INFN Laboratori Nazionali del Sud, Catania, Italy*³*Nuclear Physics Institute, Czech Academy of Sciences, 250 68 Řež near Prague, Czech Republic*

(Received 7 January 2011; published 11 April 2011)

The R -matrix approach has proved to be very useful in extrapolating the astrophysical factor down to astrophysically relevant energies, since the majority of measurements are not available in this region. However, such an approach has to be critically considered when no complete knowledge of the reaction model is available. To get reliable results in such cases one has to use all the available information from independent sources and, accordingly, fix or constrain variations of the parameters. In this paper we present a thorough R -matrix analysis of the $^{15}\text{N}(p,\gamma)^{16}\text{O}$ reaction, which provides a path from the CN cycle to the CNO bi-cycle and CNO tri-cycle. The measured astrophysical factor for this reaction is dominated by resonant capture through two strong $J^\pi = 1^-$ resonances at $E_R = 312$ and 962 keV and direct capture to the ground state. Recently, a new measurement of the astrophysical factor for the $^{15}\text{N}(p,\gamma)^{16}\text{O}$ reaction has been published [P. J. LeBlanc *et al.*, *Phys. Rev. C* **82**, 055804 (2010)]. The analysis has been done using the R -matrix approach with unconstrained variation of all parameters including the asymptotic normalization coefficient (ANC). The best fit has been obtained for the square of the ANC $C^2 = 539.2 \text{ fm}^{-1}$, which exceeds the previously measured value by a factor of ≈ 3 . Here we present a new R -matrix analysis of the Notre Dame–LUNA data with the fixed within the experimental uncertainties square of the ANC $C^2 = 200.34 \text{ fm}^{-1}$. Rather than varying the ANC we add the contribution from a background resonance that effectively takes into account contributions from higher levels. Altogether we present ten fits, seven unconstrained and three constrained. For the unconstrained fit with the boundary condition $B_c = S_c(E_2)$, where E_2 is the energy of the second level, we get $S(0) = 39.0 \pm 1.1 \text{ keVb}$ and normalized $\bar{\chi}^2 = 1.84$, i.e., the result which is similar to LeBlanc *et al.* From all our fits we get the range $33.1 \leq S(0) \leq 40.1 \text{ keVb}$ which overlaps with the result of LeBlanc *et al.* We address also the physical interpretation of the fitting parameters.

DOI: [10.1103/PhysRevC.83.044604](https://doi.org/10.1103/PhysRevC.83.044604)

PACS number(s): 26.20.-f, 24.30.-v, 25.40.Lw, 29.85.-c

I. INTRODUCTION

Nuclear data are important input into nuclear astrophysics. When resonances contribute, the analysis of the data usually is done within the R -matrix approach. The R -matrix analysis includes fitting parameters, like particle and radiative reduced widths, resonance energies, channel radii, and boundary conditions. Often nonresonant processes also contribute to the reaction mechanism. For example, the radiative capture amplitude in the R -matrix approach consists of three terms: the internal resonance amplitude, which describes the radiative capture as the process in which the incident particle penetrates through the barrier into the internal region of a target, from which radiative decay to lower lying levels occurs; the external resonance amplitude describing the formation of the resonance in the external region of target with subsequent γ decay; and the nonresonant direct capture amplitude, which describes the transition from the initial continuum to a bound state by emitting γ without formation of resonance. This nonresonant term in the R -matrix approach is contributed only by the matrix element in the external region, i.e., at distances larger than the channel radius, because the internal part of the nonresonant amplitude is included in the internal resonance amplitude. The normalization of the last two amplitudes is governed by the asymptotic normalization coefficient (ANC), which has been introduced into analysis of nuclear astrophysical data by one of us (A.M.M.) [1,2]. The ANC is a fundamental nuclear

characteristic of bound states [3] and for resonances the partial resonance width is also expressed in terms of the ANC [4,5]. The residue of the scattering S matrix in the corresponding bound state or resonance pole is expressed in terms of the ANC [4], which provides a model-independent definition of the ANC. Moreover, the ANC is the only model-independent information, which can be extracted from nuclear reactions [6]. The ANC can be determined, for example, from peripheral transfer reactions and has been extensively used in the analysis of many important astrophysical reactions [7–13].

Thus the presence of the external resonant and nonresonant direct radiative captures adds an additional parameter into the R -matrix fit, which is of fundamental importance for nuclear reactions and nuclear structure [2,3,14]. Usually the astrophysical factor (or, equivalently, the reaction cross section) is obtained from the R -matrix analysis by unconstrained variations of the fitting parameters until a minimum of $\bar{\chi}^2 = \chi^2/N$ is reached, where N is the number of degrees of freedom, i.e., the number of the data points included into the fit minus the number of the fitting parameters. However, each researcher faces a question: whether a minimum of $\bar{\chi}^2$ is always an acceptable fit which provides reliable physical parameters and correct astrophysical factor. We believe the answer would be “yes” if the reaction model is complete, i.e., all the reaction mechanisms are taken into account. However, in practice it is hardly possible. Sometimes missing reaction

mechanisms may not be important, i.e., their contribution is less than or comparable with the experimental uncertainties, sometimes it is not the case and even small contributions from missing reaction mechanisms may be important, especially when they do interfere with the reaction amplitudes, which are explicitly taken into account. In this case the fit providing the minimum of $\tilde{\chi}^2$ may be misleading because the missing reaction mechanisms are compensated by adopting unphysical parameters. What are the best general prescriptions when one uses the R -matrix fit? First, invoke all available reliable physical information from independent sources to constrain the number of fitting parameters or the interval in which they can be varied. We call it a constrained fit. Second, it is always wise to add a background contribution when one sees that a minimum of $\tilde{\chi}^2$ cannot be reached without a background if parameters are within physical boundaries. R -matrix formalism provides a solid way to take effectively into account the missing reaction mechanism. Usually, in the R -matrix approach, the cumulative effect of the higher lying distant levels is taken into account as a background [15]. Sometimes, direct mechanisms, which have smooth energy behavior, are also included in the background. What to take into account explicitly or as a background depends on the energy behavior of the corresponding amplitude and its magnitude. Since the final purpose in the analysis of astrophysical nuclear reactions is to provide reliable information for nuclear astrophysics we have to be sure that all the useful independent data have been included into analysis. Definitely the most reliable information can be obtained if one performs simultaneous R -matrix fits in all the open channels or uses available information, which has been obtained from an analysis of other open channels. This information allows us to fix or constrain reduced widths in some open channels. Since the ANC's in many cases are now available from independent experimental data or theoretical calculations [14], it is always important to fix or significantly constrain the variation of the ANC. A serious disagreement between the ANC found from the R -matrix fit and the experimentally determined one might signal that some physical input is missing in the reaction model and this incomplete knowledge is compensated for by adopting an unphysical value of the ANC.

A very instructive example is the notorious analysis of the $^{14}\text{N}(p, \gamma)^{15}\text{O}$ reaction for transition to the ground state, where the nonresonant capture contribution is also controlled by the ANC for the $^{15}\text{O}(\text{g.s.}) \rightarrow ^{14}\text{N} + p$ [9,16]. The best fit is achieved at $C \approx 11 \text{ fm}^{-1/2}$, but this fit was not accepted because the recommended ANC value is $7.4 \pm 0.5 \text{ fm}^{-1/2}$ [9,16]. The recommended in [16] $S(0) = 0.27 \pm 0.05 \text{ keVb}$ factor corresponds to the fit with the recommended ANC but the expanded uncertainty is not due to the best fit at higher ANC but to a possible contribution of the capture to the channel spin $I = 1/2$, which interferes with the 259 keV resonance. It is an important example when missing physics is taken into account rather than an unconstrained variation of the ANC, which demonstrates that it is important to keep track on the boundaries of variation of the fitting parameters in accordance with the pre-

viously available information about them obtained from other sources.

As a practical application of the procedures described above in this paper, we analyze the astrophysical $^{15}\text{N}(p, \gamma)^{16}\text{O}$ reaction, which provides the path to form ^{16}O in stellar hydrogen burning, thus transforming the CN cycle into the CNO bi-cycle and CNO tri-cycle. In stellar environments, the $^{15}\text{N}(p, \gamma)^{16}\text{O}$ reaction proceeds at very low energies, where it is dominated by the resonant capture to the ground state through the first two interfering $J^\pi = 1^-$ s -wave resonances at $E_R = 312$ and 962 keV , where E_R is the resonance energy in the center-of-mass system. There is also a small contribution from direct capture to the ground state of ^{16}O , which turns out to play an important role due to the interference with the resonant amplitudes. In our previous paper [13], the measurement of the ANC for the $^{16}\text{O} \rightarrow ^{15}\text{N} + p$ was reported. This ANC has been used to fix the nonresonant contribution to the $^{15}\text{N}(p, \gamma)^{16}\text{O}$ capture and we found that it was impossible to fit the low-energy data from [17]. Moreover, we underscored that to fit these experimental data one needs to increase the ANC almost by an order of magnitude. Our calculated astrophysical factor using the two-level, two-channel R -matrix approach led to $S(0) = 36.0 \pm 6.0 \text{ keVb}$, which is significantly smaller than $S(0) = 64 \pm 6 \text{ keVb}$ reported in [17] but in agreement with the older measurements in [18]. Correspondingly, we have found that for every 2200 ± 300 cycles of the main CN cycle, one CN catalyst is lost due to the $^{15}\text{N}(p, \gamma)^{16}\text{O}$ reaction, rather than for every 1200 ± 100 cycles determined from data of Ref. [17]. Our results were confirmed later by [19]. Recently, two new measurements of the astrophysical factor for the $^{15}\text{N}(p, \gamma)^{16}\text{O}$ have been published. The first measurement was performed at the LUNA underground accelerator facility at the Gran Sasso laboratory [20]. This measurement covered only the low-energy region, $E \leq 230 \text{ keV}$, where E is the relative $^{15}\text{N} - p$ energy. The second study of $^{15}\text{N}(p, \gamma)^{16}\text{O}$, which was just reported in [21], was performed over a wide energy range at the Notre Dame Nuclear Science Laboratory (NSL) and the LUNA II facility. The obtained $S(0) = 39.6 \pm 2.6 \text{ keVb}$ is in a perfect agreement with our prediction $S(0) = 36.0 \pm 6.0 \text{ keVb}$ [13]. However, in the R -matrix fitting of the experimental data, the ANC was used as an unconstrained fitting parameter and the best fit with the normalized $\tilde{\chi}^2 = 1.80$ was achieved for the square of the ANC $C^2 = 539 \pm 138 \text{ fm}^{-1}$, which is significantly higher than our measured value $C^2 = 192 \pm 26 \text{ fm}^{-1}$. Significant deviation of the ANC obtained in [21] signals that some physical input is missing in the reaction model and this incomplete knowledge is compensated for by adopting an unphysical value of the ANC. In the case under consideration, in the R -matrix approach, the ANC determines the overall normalization of the nonresonant radiative capture amplitude and the channel (external) part of the radiative width amplitudes of both resonances involved. Although the nonresonant amplitude is small and any sizable impact on the astrophysical factor can be achieved only by a significant variation of the ANC, the contribution of the nonresonant amplitude increases toward low energies, which is the region of the astrophysical interest.

It is the goal of this paper to demonstrate that the fit providing the minimum of $\tilde{\chi}^2$ is not always acceptable from the point of view of physics. We will show that, using the experimentally measured ANC, we can achieve the same or even better fits than in [21] by adding the background resonance, which takes effectively into account the cumulative contributions from distant 1^- levels. Our result confirms that the unphysical value of the ANC obtained in [21] is the result of neglecting the background contribution. Results of our fits are compared with the one presented in [21], which was obtained using the AZURE R -matrix code [22], and it is demonstrated that some parameters of the fit in [21] significantly deviate from those found previously. Also the constrained fits, where the observable particle widths are consistent with the previous fits of the $^{15}\text{N}(p, \alpha)^{16}\text{C}$ reaction, are presented. We demonstrate how a thorough R -matrix analysis should be done often applying the procedures used by Barker [19]. Eventually we obtained a wider interval for $S(0)$ than in [21] and indicate a still-existing inconsistency in parameters of two 1^- resonances of ^{16}O .

II. ANC

We start with the physical meaning of the ANC, which is an important input in the analysis of astrophysical reactions. As we have underscored, in the R -matrix approach the ANC determines the normalization of the external nonresonant radiative capture amplitude and the channel radiative reduced width amplitude [8]. In a single-particle approach, the nucleon ANC can be expressed in terms of the spectroscopic factor and the single-particle bound-state wave function of the nucleon calculated in some adopted mean field:

$$C^2 = S b^2, \quad (1)$$

where S is the spectroscopic factor and b is the single-particle ANC, i.e., the amplitude of the tail of the single-particle bound-state wave function. Note that the isospin Clebsch-Gordan coefficient is absorbed in the spectroscopic factor. For simplicity, we omit the quantum numbers characterizing the nucleon bound state. In such an approach we can consider the ground state of ^{16}O as the bound state ($^{15}\text{N } p$) with the proton occupying the single-particle orbital $1p_{1/2}$. The spectroscopic factor shows the probability of this configuration in the ground state of ^{16}O . Due to the identity of nucleons this probability can be larger than one. In a simple independent particle shell model the spectroscopic factor of the $1p_{1/2}$ state is equal to the number of protons occupying this orbital, i.e., 2. To determine the spectroscopic factor from Eq. (1) one needs to determine the proton bound-state wave function. To this end we adopt the Woods-Saxon potential with the standard geometry, $r_0 = 1.25$ fm and diffuseness $a = 0.65$ fm, and the spin-orbit potential depth of 6.39 MeV. Assuming that the proton is in the $p_{1/2}$ orbital we obtain the single-particle proton ANC $b \approx 9.96$ fm $^{-1/2}$. If one adopts the ANC from [21], we obtain the spectroscopic factor $S = 5.44$ vs $S = 2.1$ obtained from our $C^2 = 192$ fm $^{-1}$. Even if we adopt an unrealistically large radius $r_0 = 1.50$ fm and $a = 0.65$ fm for the Woods-Saxon potential, we obtain $b = 13.6$ fm $^{-1/2}$ and a too high spectroscopic factor $S = 2.81$.

Definitely such a high spectroscopic factor obtained from the ANC adopted in [21] requires a physical interpretation. In this aspect it would be useful to present the phenomenological spectroscopic factors obtained from the analysis of different reactions. For example, the spectroscopic factor deduced from the analysis of the $^{16}\text{O}(e, e' p)^{15}\text{N}$ reaction is $S = 1.27 \pm 0.13$ [23,24]. The proton bound-state wave function deduced from the $(e, e' p)$ reaction is reproduced by the Woods-Saxon potential with the geometry $r_0 = 1.37$ fm and $a = 0.65$ fm. The single-particle ANC of this bound-state wave function is $b = 11.62$ fm $^{-1/2}$. Using the upper limit of the deduced spectroscopic factor $S = 1.40$ we obtain the square of the proton ANC in the ground state of ^{16}O $C^2 = 189$ fm $^{-1}$, which is in a perfect agreement with our result [13]. In our paper [13], we presented the spectroscopic factors extracted from different $^{15}\text{N}(^3\text{He}, d)^{16}\text{O}$ reactions including our result. Besides our spectroscopic factor $S = 2.1$ [13], three other measurements (see references in [13]) gave $S \leq 1.76$. The DWBA reanalysis of the $^{16}\text{O}(d, ^3\text{He})^{15}\text{N}$ reaction [25] performed in [24] using the proton bound-state wave function obtained from the $^{16}\text{O}(e, e' p)^{15}\text{N}$ reaction with $r_0 = 1.37$ fm and $a = 0.65$ fm gave an even lower spectroscopic factor $S = 1.02$. With this low spectroscopic factor we get $C^2 \approx 140$ fm $^{-1}$. Since the measurements in [25] were done in 1967, the accuracy of the absolute normalization of the differential cross section in [25] might be questionable. Spectroscopic factors below 2 have also been obtained in microscopic calculations [26,27]. Concluding this discussion, we cannot find any justification for such a high value of the ANC used in [21] because it leads to an unphysical spectroscopic factor. We only can come to the conclusion that a broad variation of the ANC beyond of the experimental limits has been used in [21] to compensate for missing mechanisms in the reaction model.

III. R MATRIX

To underscore the role of the ANC in the fitting of experimental data, in this section we present the expression for the astrophysical factor in the R -matrix approach, which we use for the analysis of the experimental data. An important advantage of our code is that it provides both internal and channel (external) radiative reduced widths amplitudes. Since the external radiative width amplitude is normalized in terms of the ANC its sign is synchronized with the sign of the nonresonant amplitude, which is also expressed in terms of the ANC. Hence, the interference pattern is determined by the relative sign of the internal and external resonance amplitudes and this sign can be considered as a fitting parameter. It is a two-level, two-channel R -matrix, which includes the coherent contribution from two 1^- resonances and nonresonant term describing direct capture. The ANC determines the normalization of the nonresonant capture amplitude, which describes the external direct capture in the R -matrix approach and the channel radiative width amplitude, which are important for the fitting. But, in addition to [21], we add the coherent contribution from a background resonance rather than varying the ANC. We can assume that this background pole takes effectively into account contributions from distant levels with

$J^\pi = 1^-$. The expression for the astrophysical factor in the R -matrix method for the case under consideration can be written as [15,28]

$$S(E)(\text{keVb}) = \frac{\pi \lambda_N^2}{2} \frac{\hat{J}_R}{\hat{J}_x \hat{J}_A} \frac{m_x + m_A}{m_x m_A} 931.5^2 e^{2\pi \eta} 10 \times \left[\sum_{\nu, \tau=1,2} (\Gamma_{\nu\gamma(\text{int})}^{1/2} \pm \Gamma_{\nu\gamma(\text{ext})}^{1/2}) [\mathbf{A}^{-1}]_{\nu\tau} \Gamma_{\tau p}^{1/2} \pm M_{\text{DC}} + M_{\text{BG}} \right], \quad (2)$$

where $\lambda_N = 0.2118$ fm is the nucleon Compton wavelength, 931.5 is the atomic mass unit in MeV, Z_j and m_j are the charge and mass of particle j , and μ_{ij} is the reduced mass of particles i and j . η is the Coulomb parameter in the initial state of the reaction, J_j is the spin of particle j , and

J_R is the spin of the resonance, $\hat{J} = 2J + 1$. $k_\gamma = (E + \varepsilon)/(\hbar c)$ is the momentum of the emitted photon expressed in fm^{-1} , E is the relative $p - A$ energy, A is the target, ε is the proton binding energy of the bound state ($A p$), L is the multipolarity of the electromagnetic transition, \mathbf{A} is the standard level matrix for the two-channel, two-level case [15], $\Gamma_{\tau c}^{1/2} = \sqrt{2} P_{l_c}(k_c, r_c) \gamma_{\tau c}$, $\gamma_{\tau c}$ is the reduced width amplitude for the level $\tau = 1, 2$ in the channel $c = p, \alpha$. $P_{l_c}(k_c, r_c)$ is the barrier penetrability factor in the channel c , l_c is the orbital angular momentum of the resonance, and k_c is the relative momentum of the particles in the channel c . r_c is the R -matrix channel radius in the channel c , $\Gamma_{\nu\gamma(\text{int})}^{1/2} = \sqrt{2} k_\gamma^{L+1/2} \gamma_{\nu\gamma(\text{int})}$, $\gamma_{\nu\gamma(\text{int})}$ is the internal radiative reduced width amplitude for transition from the level ν to a bound state (the ground state in the case under consideration), $\Gamma_{\nu\gamma(\text{ext})}^{1/2} = \sqrt{2} k_\gamma^{L+1/2} \gamma_{\nu\gamma(\text{ext})}$, $\gamma_{\nu\gamma(\text{ext})}$ is the complex channel (external) radiative reduced width amplitude for transition from the level ν to a bound state given by the expression

$$\gamma_{\nu\gamma(\text{ext})} = C \sqrt{\frac{1}{2} \frac{e^2}{\hbar c} \lambda_N \frac{931.5}{E}} r_p^{L+1/2} \mu_{pA}^L \left[\frac{Z_p}{m_p^L} + (-1)^L \frac{Z_A}{m_A^L} \right] \sqrt{\frac{(L+1)\hat{L}}{L}} \frac{1}{\hat{L}!!} \Gamma_{\nu p}^{1/2} \sqrt{P_{l_p}(k_p, r_p)} [F_{l_p}^2(k_p, r_p) + G_{l_p}^2(k_p, r_p)] \times W_{-\eta_f, l_f+1/2}(r_p) \langle l_p 0 L 0 | l_f 0 \rangle U(L l_f J_i I; l_p J_f) \left[\text{Int}_1 + i \frac{F_{l_p}(k_p, r_p) G_{l_p}(k_p, r_p)}{k_p r_p} P_{l_p}(k_p, r_p) \text{Int}_2 \right], \quad (3)$$

$$\text{Int}_1 = \frac{F_{l_p}^2(k_p, r_p)}{k_p r_p} P_{l_p}(k_p, r_p) \int_{r_p}^{\infty} dr \frac{r^L}{r_p^{L+1}} \frac{W_{-\eta_f, l_f+1/2}(r)}{W_{-\eta_f, l_f+1/2}(r_p)} \frac{F_{l_p}(k_p, r)}{F_{l_p}(k_p, r_p)} + \frac{G_{l_p}^2(k_p, r_p)}{k_p r_p} P_{l_p}(k_p, r_p) \int_{r_p}^{\infty} dr \frac{r^L}{r_p^{L+1}} \frac{W_{-\eta_f, l_f+1/2}(r)}{W_{-\eta_f, l_f+1/2}(r_p)} \frac{G_{l_p}(k_p, r)}{G_{l_p}(k_p, r_p)}, \quad (4)$$

$$\text{Int}_2 = \int_{r_p}^{\infty} dr \frac{r^L}{r_p^{L+1}} \frac{W_{-\eta_f, l_f+1/2}(r)}{W_{-\eta_f, l_f+1/2}(r_p)} \frac{F_{l_p}(k_p, r)}{F_{l_p}(k_p, r_p)} - \int_{r_p}^{\infty} dr \frac{r^L}{r_p^{L+1}} \frac{W_{-\eta_f, l_f+1/2}(r)}{W_{-\eta_f, l_f+1/2}(r_p)} \frac{G_{l_p}(k_p, r)}{G_{l_p}(k_p, r_p)}, \quad (5)$$

$F_{l_p}(k_p, r)$ and $G_{l_p}(k_p, r)$ are the Coulomb regular and singular solutions, $W_{-\eta_f, l_f+1/2}(r)$ is the Whittaker function describing the radial dependence of the tail of the bound state wave function to which transition occurs after the photon is emitted. η_f is the Coulomb parameter of the bound state and l_f its orbital angular momentum, $\langle l_p 0 L 0 | l_f 0 \rangle$ is the Clebsch-Gordan coefficient, and $U(L l_f J_i I; l_p J_f)$ is the normalized Racah coefficient. J_i is the total angular momentum of the system $p + A$ in the initial state of the radiative capture process, which is equal to the resonance spin, $J_i = J_R$, I is the channel spin. The nonresonant capture amplitude describing the external direct capture in the R -matrix method is given by

$$M_{\text{DC}} = 2C \sqrt{\frac{e^2}{\hbar c} \lambda_N \frac{931.5}{E}} (k_\gamma r_p)^{L+1/2} \mu_{pA}^L \left[\frac{Z_p}{m_p^L} + (-1)^L \frac{Z_A}{m_A^L} \right] \sqrt{\frac{(L+1)\hat{L}}{L}} \frac{1}{\hat{L}!!} \sqrt{P_{l_p}(k_p, r_p)} \times W_{-\eta_f, l_f+1/2}(r_p) F_{l_p}(k_p, r_p) G_{l_p}(k_p, r_p) \langle l_p 0 L 0 | l_f 0 \rangle U(L l_f J_i I; l_p J_f) \text{Int}_2. \quad (6)$$

As we can see the channel radiative width amplitudes and the direct (nonresonant) capture amplitude are proportional to the same ANC because both describe the peripheral processes contributed by the tail of the overlap function (in the case under consideration it is $\langle \varphi_{i5N} | \varphi_{i6O} \rangle$), where φ_i is the bound state wave function of nucleus i , whose amplitude is the ANC. Besides, the channel radiative width amplitude $\gamma_{\nu\gamma(\text{ext})}$ contains the proton reduced width amplitude $\gamma_{\nu p}$. Hence the relative sign of $\gamma_{\nu\gamma(\text{ext})}$ and M_{DC} depends on the sign of $\gamma_{\nu p}$. It is also worth mentioning that $\gamma_{\nu\gamma(\text{int})}$ is a fitting parameter and

$\gamma_{\nu\gamma(\text{ext})}$ is a complex quantity because it contains an imaginary part. The radiative width is given by equation

$$\Gamma_{\nu\gamma} = |\Gamma_{\nu\gamma(\text{int})}^{1/2} - \Gamma_{\nu\gamma(\text{ext})}^{1/2}|^2 = 2k_\gamma^3 |\gamma_{\nu\gamma(\text{int})} - \gamma_{\nu\gamma(\text{ext})}|^2 \quad (7)$$

calculated at the ν th resonance energy. Another important point to underscore is that the signs of $\Gamma_{\nu\gamma(\text{ext})}^{1/2}$ and M_{DC} relative to $\Gamma_{\nu\gamma(\text{int})}^{1/2}$ are synchronized. In all the fits presented below we use a positive sign because it gives a better fit.

Finally the background resonance amplitude can be written as

$$M_{(\text{BG})} = \frac{\Gamma_{\gamma(\text{BG})}^{1/2} \Gamma_{p(\text{BG})}^{1/2}}{E - E_{R(\text{BG})} + i \frac{\Gamma_{(\text{BG})}}{2}}, \quad (8)$$

where $E_{R(\text{BG})}$ is the resonance energy of the background resonance,

$$\Gamma_{\gamma(\text{BG})}^{1/2} = \sqrt{2} k_{\gamma}^{L+1/2} \gamma_{\gamma(\text{BG})}, \quad (9)$$

$$\Gamma_{c(\text{BG})}^{1/2} = \sqrt{2} P_{l_c}(k_c, r_c) \gamma_{c(\text{BG})}, \quad (10)$$

and $\gamma_{\gamma(\text{BG})}$ is a complex radiative width amplitude for the decay of the background resonance to a bound state and $\gamma_{c(\text{BG})}$ is the reduced width amplitude of the background resonance for the channel c . The total resonance width of the background resonance is given by $\Gamma_{(\text{BG})} = \Gamma_{p(\text{BG})} + \Gamma_{\alpha(\text{BG})}$, where $\Gamma_{c(\text{BG})}$ is the partial resonance width in the channel c .

Note that all the energies are in MeV but the astrophysical factor $S(E)$ is in keVb. The dimension of the reduced particle width amplitude γ_{vc} is $\text{MeV}^{1/2}$ but $\gamma_{\nu\gamma}$ has dimension $\text{MeV}^{1/2} \text{fm}^{3/2}$ for $L = 1$.

IV. ANALYSIS

Altogether we performed seven unconstrained and three constrained fits with the boundary conditions $B_c = S_c(E_2)$ and $S_c(E_1)$. First we present two fits without a background pole. Then we perform two unconstrained fits called fits $A(113)$, and two constrained fits called fits $B(113)$. In these fits we use all 113 data points of [21]. We also performed two unconstrained fits to determine the uncertainty of the parameters and the astrophysical factor when the experimental data are deviated from the center by $\pm 1\sigma$. In addition, we performed also two fits, $A(70)$ and $B(70)$, using only 70 low-energy data points of [21] in the region of the first resonance. For all the fits the channel radii in the proton and α channels are $r_p = 5.03$ fm and $r_{\alpha} = 7.0$ fm, correspondingly, and the ANC $C = 14.154 \text{ fm}^{-1/2}$ are kept the same as in [13] and [29] and the background resonance energy is fixed at $E_{R_{\text{BG}}} = 5.07$ MeV. All other parameters are varied to get a best fit. For the case under consideration $l_p = 0$, $l_f = 1$, $J_f = 0$, $J_R = 1$, and $I = 1$.

A. Fits without background resonance

We begin our R -matrix fit of the data from [21] using the reaction model, which is contributed by two 1^- resonances and nonresonant capture. This fit helps us to identify the importance of the background. In Fig. 1 we demonstrate two best fits to 113 data points of [21] without any background pole with the boundary conditions in the channel $c = p, \alpha$ $B_c = S_c(E_2)$, and $B_c = S_c(E_1)$. The best fit with $B_c = S_c(E_2)$ is achieved at $E_2 = 0.956$ MeV and $E_1 = 0.2872$ MeV and results in $S(0) = 34.2$ keVb with $\tilde{\chi}^2 = 2.6$ and total $\chi^2 = 273.1$. For the fit with $B_c = S_c(E_1)$ at $E_1 = 0.30872$ MeV and $E_2 = 1.0794$ MeV we get $S(0) = 34.6$ keVb with $\tilde{\chi}^2 = 2.5$ and $\chi^2 = 259.9$. Parameters of the

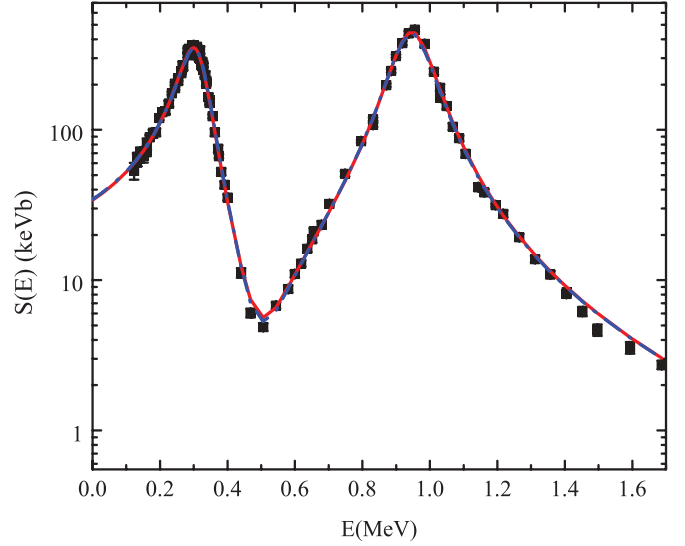


FIG. 1. (Color online) The astrophysical $S(E)$ factor for the $^{15}\text{N}(p, \gamma)^{16}\text{O}$ reaction. The black squares are experimental data from Ref. [21]. The red solid line is our unconstrained fit with the boundary condition $B_c = S_c(E_2 = 0.956 \text{ MeV})$, which takes into account three interfering amplitudes: two 1^- resonances and a nonresonant term. No background pole is included. The blue dot-dashed line is a similar fit with the boundary condition $B_c = S_c(E_1 = 0.30872 \text{ MeV})$. The ANC is $C = 14.154 \text{ fm}^{-1/2}$ as in all other fits.

fits are given in Tables I and II. The only difference from the fit presented in [21] is that we fixed the ANC at the experimentally measured value while in [21] the ANC was an unconstrained fitting parameter. As we can see both fits are quite good except for the bottom between two resonances and the high energy tail. Without the background resonance we miss just a contribution of a few keVb, which is very small compared to the resonance peaks, which are a few hundred keV. It is a straightforward indication that, by adding a small contribution from the background resonance, we can improve the fit and decrease $\tilde{\chi}^2$. If we would try to improve the fit by varying the nonresonant contribution, i.e., the ANC, then, due to very small nonresonant amplitude, we will be required to make a significant increase of the ANC. Figure 9(b) from [21] confirms this conclusion: to get down $\tilde{\chi}^2$ to the minimum one really needs to increase significantly the ANC as it has been done in [21].

B. Unconstrained fits to all the data points

Here, instead of varying the ANC to decrease $\tilde{\chi}^2$, we perform two unconstrained fits $A(113)$ to the Notre Dame-LUNA data [21] adding a background resonance. All 13 parameters except for the ANC, channel radii, and the background resonance energy are allowed to vary. Performing such fits with the fixed ANC one can compare the obtained fitting parameters with the ones determined from the analysis of other channels. To determine the resonance parameters, the fits are performed with two boundary conditions. The first boundary condition has been set up near the second resonance,

TABLE I. Resonance parameters. Parameters of the R -matrix fits to the $^{15}\text{N}(p, \gamma)^{16}\text{O}$ capture 113 data points [21] along with the fitting parameters from [21,31,32].

Reference	γ_{1p}^2 [keV]	$\tilde{\Gamma}_{1p}$ [keV]	$\gamma_{1\alpha}^2$ [keV]	$\tilde{\Gamma}_{1\alpha}$ [keV]	$\Gamma_{1\gamma}$ [eV]	γ_{2p}^2 [keV]	$\tilde{\Gamma}_{2p}$ [keV]	$\gamma_{2\alpha}^2$ [keV]	$\tilde{\Gamma}_{2\alpha}$ [keV]	$\Gamma_{2\gamma}$ [eV]
[21]	52.8	0.20	13.5	112.0	33.8	309.1	110.6	5.0	40.6	38.7
[19], Table II, HH(c)	355.2	1.0	10.6	85.8		265.2	98	5.4	40.3	
[32], Resonances in $^{12}\text{C} + \alpha$ scattering		1.1		92 ± 8	9.5 ± 1.7		100		45 ± 18	44 ± 8
Present work, unconstrained fits										
A(113)	358.8	1.3	14.4	99.4	7.5	221.6	82.8	7.5	63.2	63.6
Present work, constrained fits										
B(113)	259.8	1.0	13.6	99.7	9.3	268.9	98.1	6.0	49.4	54.4
Present work, unconstrained fits without background resonance	353.3	1.3	14.1	98.3	7.5	231.4	86.0	6.9	58.2	57.6

while the energy of the first level is a fitting parameter. The found parameters of the second resonance are transformed using Barker's transformation [30]. After that we repeat the fit with the boundary condition near the first resonance. Using Barker's transformation [30] we get the resonance parameters of the first resonance. Such unconstrained fits will allow to check how reliable extracted parameters are by comparing them with existing results obtained from previous studies of the 1^- resonances of ^{16}O . We also compare the parameters of our fit with the ones from [21].

First we have searched for the best fit for the boundary condition $B_c = S_c(E_2)$, E_2 is the energy of the second level which is taken close to the second resonance energy $E_{R_2} = 0.9594$ MeV adopted in [21] while the first level is varied to get the best fit. We find the best fit at $E_2 = 0.956$ MeV and $E_1 = 0.1662$ MeV. The channel radii, $r_p = 5.03$ fm and $r_\alpha = 7.0$ fm, and ANC $C = 14.154$ fm $^{-1/2}$ have been used in all the fittings. The energy of the included background resonance is 5.07 MeV, the proton reduced width amplitude of the background resonance is $\gamma_{p(BG)} = -0.3$ MeV $^{1/2}$, and the α reduced width amplitude $\gamma_{\alpha(BG)} = 0.07$ MeV $^{1/2}$. In the fit A(113) the search for the best fitting has been performed using an unconstrained variation of other parameters. Using Barker's transformation [22,30] the fitting parameters are transformed to the ones corresponding to the boundary condition at the second resonance energy $E_{R_2} = 0.9594$ MeV adopted in [21].

These parameters are given as the fitting parameters for the second resonance in Tables I and II. The radiative width for the background pole is found to be $\Gamma_{\gamma(BG)} = 354.9$ eV. After that we can find the observable partial resonance widths for the channel c using the standard R -matrix equation [19]

$$\tilde{\Gamma}_{\nu c} = \frac{2\gamma_{\nu c}^2 P_c(E_{R_\nu}, r_c)}{1 + \sum_{c'=p,\alpha} \gamma_{\nu c'}^2 \frac{dS_{c'}}{dE} \Big|_{E=E_{R_\nu}}}, \quad (11)$$

where E_{R_ν} is the resonance energy of the level ν and $\tilde{\Gamma}_{\nu c}$ is the observable partial width of the level ν in the channel c .

In the second unconstrained fit A(113), we have searched for the best fit with the boundary condition $B_c = S_c(E_1)$, where the energy of the first level E_1 is near the first resonance at $E_{R_1} = 0.3104$ MeV adopted in [21] while the second level is varied to get the best fit. For this boundary condition we find the best fit at $E_1 = 0.30872$ MeV and $E_2 = 1.0576$ MeV. The fitting parameters are transformed to the ones corresponding to the boundary condition at the first resonance $E_{R_1} = 0.3104$ MeV adopted in [21] and are shown in Tables I and II as the fitting parameters for the first resonance. To get the observable widths we use Eq. (11). The radiative width for the background pole is found to be $\Gamma_{\gamma(BG)} = 360.5$ eV. In Fig. 2 we demonstrate the astrophysical factors $S(E)$ obtained from these two unconstrained A(113) fits with fixed ANC $C = 14.154$ fm $^{-1/2}$ and the background resonance

TABLE II. Internal and external radiative width amplitudes for the first and second resonances. The amplitudes for the second resonance at $E_{R_2} = 0.9594$ MeV (first resonance at $E_{R_1} = 0.3104$ MeV) are determined from the unconstrained fit A(113) and constrained fit B(113) for the boundary condition at the second (first) resonance.

Fits	$\gamma_{1\gamma(\text{int})}$ [MeV $^{1/2}$ fm $^{3/2}$]	$\gamma_{1\gamma(\text{ext})}$ [MeV $^{1/2}$ fm $^{3/2}$]	$\gamma_{2\gamma(\text{int})}$ [MeV $^{1/2}$ fm $^{3/2}$]	$\gamma_{2\gamma(\text{ext})}$ [MeV $^{1/2}$ fm $^{3/2}$]
[21]	0.22		0.19	
[19]	0.085		0.24	
Unconstrained fits A(113)	0.062	$0.061 + i 0.000059$	0.28	$0.053 + i 0.0041$
Constrained fits B(113)	0.085	$0.052 + i 0.000054$	0.25	$0.059 + i 0.0044$
Unconstrained fits without background resonance	0.062	$0.060 + i 0.000059$	0.26	$0.055 + i 0.0042$

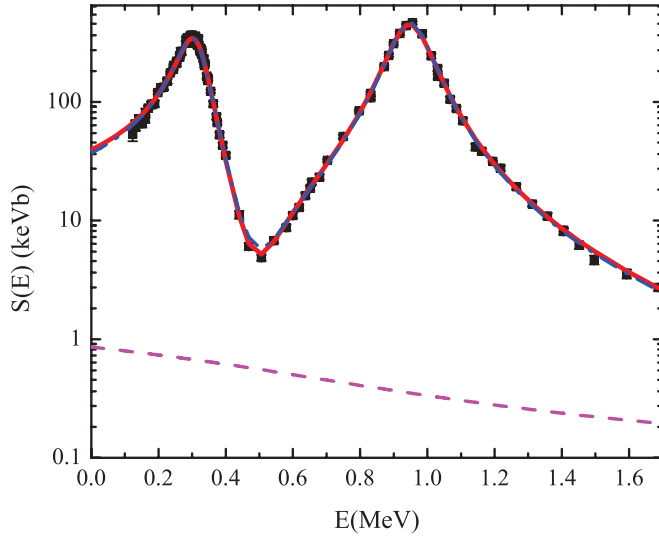


FIG. 2. (Color online) The astrophysical $S(E)$ factor for the $^{15}\text{N}(p, \gamma)^{16}\text{O}$ reaction. The black squares are experimental data from Ref. [21]. The red solid line is our unconstrained R -matrix fit $A(113)$ with the boundary condition $B_c = S_c(E_2)$, which takes into account four interfering amplitudes: two 1^- resonances, a nonresonant term, and background resonance at 5.07 MeV. The blue dot-dashed line is our unconstrained R -matrix fit $A(113)$ similar to the previous one but with the boundary condition $B_c = S_c(E_1)$. The magenta dashed line is the nonresonant $S(E)$ factor for the ANC $C = 14.154 \text{ fm}^{-1/2}$.

included. The red solid line is the fit corresponding to the boundary condition at $E_2 = 0.956 \text{ MeV}$ with the normalized $\bar{\chi}^2 = 1.84$. This fit is practically identical to the one in [21] resulting in $S(0) = 39.0 \text{ keVb}$ in agreement with [21]. For the fit $A(113)$ with the boundary condition at $E_1 = 0.30872$, the blue dotted-dashed line, we obtain $\bar{\chi}^2 = 1.76$ with $S(0) = 37.2 \text{ keVb}$. This fit goes slightly lower than the red line at low energies, better reproducing the low-energy trend of the data. The magenta dashed line represents the nonresonant $S(E)$ factor for the ANC $C = 14.154 \text{ fm}^{-1/2}$ which has been used for both fits. This ANC is within the experimental interval $13.86 \pm 0.91 \text{ fm}^{-1/2}$ determined from the $^{15}\text{N}(^3\text{He}, d)^{16}\text{O}$ reaction [13]. Thus adopting a physical ANC we correctly fix the normalization of the external direct capture amplitude and the channel radiative width amplitude, and adding the background pole rather than varying the ANC way

beyond experimental limits [21] we are able to get the same fit as in [21]. The obtained formal reduced widths and observable resonance widths for the fits $A(113)$ along with the corresponding parameters from [21,31,32] are given in Tables I and II.

We can now compare the results of the fits $A(113)$ with [21,19], and resonance parameters obtained from $^{12}\text{C} + \alpha$ scattering [32]. The last datum should be quite accurate, especially for the first resonance. Note that from different fits presented in [19] we choose the fit $HH(c)$, Tables II and III, to the data of [18], because they are pretty close to the data of [21] in the region of the first resonance and the selected fit from [19] resulted in $S(0) = 35.2 \text{ keVb}$, which agrees with our results and is close to [21] $S(0) = 39.6 \pm 2.6 \text{ keVb}$. As it has been mentioned in [19], there is a significant uncertainty in the values of the proton and α partial widths for the second resonance what can also be concluded from compilation [32]. That is why there are no recommended values for these widths in [19] after an analysis of the $^{15}\text{N}(p, \alpha)^{12}\text{C}$ data. One of the problems is that the $^{15}\text{N}(p, \alpha)^{12}\text{C}$ and $^{15}\text{N}(p, \gamma)^{16}\text{O}$ reactions put a limitation on the ratio $\gamma_{1\alpha}^2/\gamma_{2\alpha}^2$ and the $E1$ strength ratio of the second and first resonances, which should be equal due to the isospin mixture of two 1^- resonances. This isospin mixture can be written as [17–19]

$$\begin{aligned} \psi_1 &= \alpha |T = 0\rangle + \beta |T = 1\rangle, \\ \psi_2 &= \beta |T = 0\rangle - \alpha |T = 1\rangle, \end{aligned} \quad (12)$$

where $\alpha^2 + \beta^2 = 1$. Since the α -particle decays of these resonances in ^{16}O to the ground state are allowed only due to the $T = 0$ components, we have

$$\frac{\gamma_{1\alpha}^2}{\gamma_{2\alpha}^2} = \frac{\alpha^2}{\beta^2}. \quad (13)$$

Correspondingly, the strength of the $E1$ decays of these resonances to the ground state is entirely determined by $T = 1$, i.e.,

$$\frac{E1_2}{E1_1} = \frac{\alpha^2}{\beta^2}. \quad (14)$$

From the fit in [21] one gets the ratio $\gamma_{1\alpha}^2/\gamma_{2\alpha}^2 = 2.7$ and $\gamma_{1\alpha}^2/\gamma_{2\alpha}^2 = 1.96$ from [19]. To get the ratio of the $E1$ intensities we remind the reader that $\gamma_{\nu\gamma(\text{int})} \sim \langle \varphi_p | \hat{O} | \psi_{\nu(\text{int})} \rangle |_{r \leq r_p}$, \hat{O} is the electromagnetic operator, φ_p is the proton bound-state wave function in ^{16}O and $\psi_{\nu(\text{int})}$ is the internal resonant

TABLE III. Resonance parameters. Parameters of the unconstrained $A(70)$ and constrained $B(70)$ fits to the 70 data points of the $^{15}\text{N}(p, \gamma)^{16}\text{O}$ process [21]. Physical meaning of the parameters and the procedure are similar to the one described in the caption for Table I. Note that for both fits $A(70)$ and $B(70)$ we present the parameters only for the first resonance because the boundary condition is adopted at the energy of the first level.

Fit	γ_{1p}^2 [keV]	$\tilde{\Gamma}_{1p}$ [keV]	$\gamma_{1\alpha}^2$ [keV]	$\tilde{\Gamma}_{1\alpha}$ [keV]	$\Gamma_{1\gamma}$ [eV]
fit $A(70)$, $B_c = S_c(E_1 = 0.30872 \text{ MeV})$	358.9	1.4	14.3	98.9	6.9
fit $B(70)$, $B_c = S_c(E_1 = 0.30872 \text{ MeV})$	260.2	1.0	13.6	99.7	9.0

wave function of the ν th resonance given by a standing wave satisfying Eq. (12). Then the ratio of the $E1$ intensities can be estimated from the ratio of $\gamma_{\nu\gamma(\text{int})}^2$ assuming the dominance of the internal contribution to the electromagnetic transition matrix element. From [21] we get $\gamma_{2\gamma(\text{int})}^2/\gamma_{1\gamma(\text{int})}^2 = 0.66$ and $\gamma_{2\gamma(\text{int})}^2/\gamma_{1\gamma(\text{int})}^2 = 7.97$ from [19]. If we use the $E1$ intensity ratio of the total radiative widths we get from [21] $E1_2/E1_1 = (\Gamma_{2\gamma}/k_{2\gamma}^3)/(\Gamma_{1\gamma}/k_{1\gamma}^3) = 0.98$, where $k_{\nu\gamma} = (E_{R_\nu} + \varepsilon)/\hbar c$ is the momentum of the emitted photon for transition from the resonance ν with the resonance energy E_{R_ν} to the ground state with the proton binding energy ε . Thus the ratio of the α -reduced widths from [21] is reasonably consistent with findings in [19,29], while the ratio of the radiative resonance widths is too small compared to all the previous estimations due to too high radiative width of the first resonance which was estimated to be around 10 eV [18,32,33]. The proton partial width $\tilde{\Gamma}_{2p} = 110$ keV in [21] is higher than the previous estimations [19,31,32], while our 82.8 keV is lower. Note that we do not include estimations from the analysis of the data of [17].

The partial widths for the first resonance are better known than for the second one. According to [19] and [31], $\tilde{\Gamma}_{1p} = 1.1$ keV and 1.0 keV, correspondingly, and $\tilde{\Gamma}_{1\alpha} = 92 \pm 8$ keV and different previous estimations are pretty close to these values [32]. Note that all the widths are in the center-of-mass system. All three partial widths obtained in [21] disagree with other results, in particular, with the $^{12}\text{C} + \alpha$ resonance scattering data [32]. It is impossible to explain a too low value of $\tilde{\Gamma}_{1p} = 0.2$ keV and too high values of $\Gamma_{1\gamma} = 33.8$ eV and $\tilde{\Gamma}_{1\alpha} = 112$ keV [21], which are beyond the boundaries of the existing estimations. Our unconstrained fits $A(113)$ are not satisfactory also, although they better agree with the previous estimations for the first resonance. The quoted value $\Gamma_{1\gamma} = 12 \pm 2$ eV in [32] was taken from [17], while [18] obtained from a single level analysis (only the first resonance was included) that $\Gamma_{1\gamma} = 8$ eV, and from the two-level analysis $\Gamma_{1\gamma} = 12.8$ eV. Our $\Gamma_{1\gamma} = 7.5$ eV is significantly lower than the corresponding value in [21], but agrees with $\Gamma_{1\gamma} = 9.5 \pm 1.7$ eV determined from the $^{12}\text{C} + \alpha$ resonance scattering [32] and pretty close to other estimations [18,33]. However, our $\Gamma_{2\gamma} = 63.6$ eV is higher than $\Gamma_{2\gamma} = 32 \pm 5$ eV [33], 38.7 eV [21], and 44 ± 8 eV obtained from the branching ratio [32] but lower than 88 eV [18]. Our $\tilde{\Gamma}_{1\alpha} = 99.4$ keV is in a perfect agreement with the estimation 92 ± 8 keV [19] and with other estimations [32]. However, our $\gamma_{1\alpha}^2/\gamma_{2\alpha}^2 = 1.92$ is much smaller than $(\Gamma_{2\gamma}/k_{2\gamma}^3)/(\Gamma_{1\gamma}/k_{1\gamma}^3) = 7.2$.

Thus unphysical ANC in [21] leads inevitably to significant deviations of other resonance parameters, especially for the first resonance, while our unconstrained fits with correct ANC produce better resonance parameters, although they are also not perfect.

C. Constrained fits to all data points

Due to the above-mentioned problems with the unconstrained fits $A(113)$ we performed two constrained fits $B(113)$. The goal of these fits is to demonstrate that fixing some

parameters at values obtained from previous works, we still can get as good fits as unconstrained ones but with better physical parameters.

Once again we did two different fits corresponding to two boundary conditions with parameters given in Tables I and II. In the constrained fits $B(113)$ the procedure is the same as described before for the unconstrained fits. In these fits, in addition to the fixed channel radii in the proton and α channels, $r_p = 5.03$ fm and $r_\alpha = 7.0$ fm, the ANC $C = 14.154$ fm $^{-1/2}$ and the background resonance energy $E_{R_{BG}} = 5.07$ MeV, we also fix $\gamma_{\nu c}$, $c = p, \alpha$, when the boundary condition is chosen near the resonance energy E_{R_ν} . These reduced widths are taken from the analysis of the direct $^{15}\text{N}(p, \alpha)^{12}\text{C}$ data [19,29,33] and indirect Trojan Horse data [29]. First, we adopt the boundary condition near the second resonance at $E_2 = 0.956$ MeV with the energy of the first level $E_1 = 0.170$ MeV. For the best fit we get $\tilde{\chi}^2 = 1.93$ and $S(0) = 38.8$ keVb. The radiative width for the background pole is found to be $\Gamma_{\gamma(\text{BG})} = 129.3$ eV.

To determine the parameters for the first resonance we use the boundary condition $B_c = S_c(E_1)$ near the first resonance $E_1 = 0.30872$ MeV and found from the fit the second energy level $E_2 = 1.0576$ MeV. The rest is the same as in fit $A(113)$. The radiative width for the background resonance is $\Gamma_{\gamma(\text{BG})} = 283.1$ eV. For the best constrained fit with the boundary condition at the first resonance we get $S(0) = 37.2$ keVb with $\tilde{\chi}^2 = 1.74$. We note that the total χ^2 for the unconstrained fit $A(113)$ with the boundary condition $B_c = S_c(E_1)$ is slightly smaller than for the corresponding constrained fit $B(113)$. However, because for the constrained fit the number of the fitting parameters is smaller than for the unconstrained one, the normalized $\tilde{\chi}^2$ for the constrained fit is slightly smaller than for the unconstrained. The parameters given in Tables I and II are obtained for the boundary conditions at the resonance energies adopted in [21]. Barker's transformation [30] to get the fitting parameters at the energy of the first resonance practically did not change them because of the proximity of our adopted first level $E_1 = 0.30872$ MeV and the first resonance energy $E_{R_1} = 0.3104$ MeV adopted in [21]. In Fig. 3 the $S(E)$ factors are shown for both constrained fits $B(113)$. Note that the blue dot-dashed line, which gives smaller $S(0)$ than the red solid line, better reproduces the low-energy experimental trend. The constrained fits $B(113)$ have parameters which better agree with the previous estimations [19,32] than unconstrained fits $A(113)$. In particular, $\tilde{\Gamma}_{2\alpha}$ is lower and agrees with the $^{12}\text{C} + \alpha$ analysis [32]. All other observable partial widths also agree very well with the previous estimations from the analysis of different open channels [32] and, in particular, the radiative width for the first resonance is in better agreement with [32]. However, our $\Gamma_{2\gamma} = 54.4$ eV, although lower than in the fit $A(113)$, is still high and remains the only problem to get consistency with previous estimations [32]. Correspondingly, the ratio $(\Gamma_{2\gamma}/k_{2\gamma}^3)/(\Gamma_{1\gamma}/k_{1\gamma}^3) = 5.0$ is still too high compared to $\gamma_{1\alpha}^2/\gamma_{2\alpha}^2 = 2.3$ which is fixed in agreement with $^{15}\text{N}(p, \alpha)^{12}\text{C}$ [19,29]. Thus, even with the constrained fits, which prove consistent with the previous estimations, we are not able to satisfy the isospin mixing equations still having too high $\Gamma_{2\gamma}$ or too high $\gamma_{2\alpha}$.

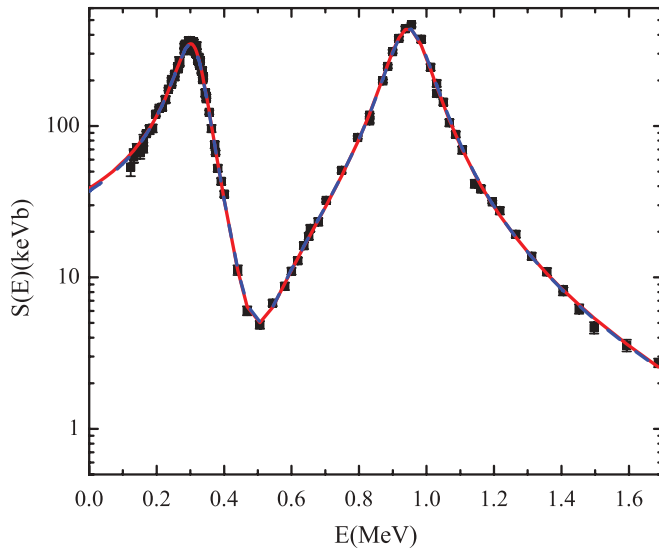


FIG. 3. (Color online) The astrophysical $S(E)$ factor for the $^{15}\text{N}(p, \gamma)^{16}\text{O}$. The red solid line is the constrained fit $B(113)$ with the boundary condition $B_c = S_c(E_2 = 0.956 \text{ MeV})$, the blue dot-dashed line is the constrained fit $B(113)$ with the boundary condition $B_c = S_c(E_1 = 0.30872 \text{ MeV})$. The black squares are experimental data from Ref. [21]. The ANC is $C = 14.154 \text{ fm}^{-1/2}$.

D. Band for unconstrained fit

In this section we estimate the uncertainty of the parameters and the astrophysical factor $S(E)$ by fitting to the lower and upper limits of the experimental data. These limits are obtained by taking into account $\pm 1\sigma$ deviation from the center of the experimental data. In Fig. 4, in the logarithmic scale for both axes, we show the band between upper and lower limits of the astrophysical factor $S(E)$ obtained from the unconstrained fit $A(113)$ with the boundary condition $B_c = S_c(E_2)$ at $E_2 = 0.956 \text{ MeV}$ for the energy region $E < 1.7 \text{ MeV}$. The upper (lower) limit with $S(0) = 40.1 \text{ keVb}$ [$S(0) = 37.9 \text{ keVb}$] and $\tilde{\chi}^2 = 3.0$ ($\tilde{\chi}^2 = 2.6$) of the band corresponds to the fitting of the experimental data which deviate by 1σ up (down) from the center which corresponds to $S(0) = 39.0 \text{ keVb}$ with $\tilde{\chi}^2 = 1.84$. Thus, taking into account the experimental uncertainties given in [21], we can conclude that our unconstrained fit $A(113)$ with the boundary condition $B_c = S_c(E_2)$ results in $S(0) = 39.0 \pm 1.1 \text{ keVb}$. However, the logarithmic scales for both axes show the problem with the fitting at low energies, where the fit $A(113)$ with the boundary condition $B_c = S_c(E_2)$ deviates from the experimental trend. A similar trend is present in the fit of [21]. The reason for this trend is that our fits and the fit in [21] have been performed minimizing the weighted χ^2 with the weights Δ_i^{-2} , where Δ_i is the experimental uncertainty at point i . Since the relative experimental uncertainties at low energies are larger than in the region between the two resonances and at higher energies, the weighted fit underestimates the importance of the low-energy region, which is the most crucial for determination of the $S(0)$ astrophysical factor.

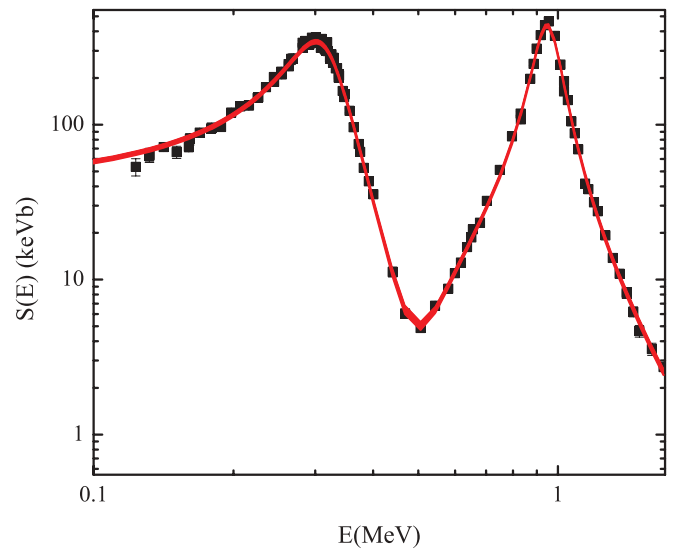


FIG. 4. (Color online) The astrophysical $S(E)$ factor for the $^{15}\text{N}(p, \gamma)^{16}\text{O}$. The band for the astrophysical factor $S(E)$ obtained from the unconstrained fit $A(113)$ with the boundary condition $B_c = S_c(E_2)$. The upper and lower limits of the band correspond to the fitting of the experimental data, which deviate by 1σ up and down from the center, correspondingly. Note that the borders of the band have practically the same particle-reduced width amplitudes $\gamma_{\nu c}$ for the first and second levels. The proton partial width for the second resonance within the band is $\tilde{\Gamma}_{2p} = 82.8 \pm 0.6 \text{ keV}$, the α -particle partial width for the second resonance $\tilde{\Gamma}_{2\alpha} = 63.2 \pm 0.9 \text{ keV}$, the radiative width of the second resonance $\Gamma_{2\gamma} = 63.6 \pm 2.4 \text{ eV}$, and the radiative width of the background pole $\Gamma_{\gamma(\text{BG})} = 354.9 \pm 23.6 \text{ eV}$. The black squares are experimental data from Ref. [21].

E. Fits to 70 data points

To increase the weight of the low-energy points we present also two fits to 70 low-energy data points in the region of the first resonance rather than to all 113 data points: the unconstrained fit $A(70)$ with $B_c = S_c(E_1)$ and the constrained fit $B(70)$ with the boundary condition $B_c = S_c(E_1)$. If the reaction model is complete, definitely only the full energy region fit makes sense. However, in the case under consideration we add the background resonance to compensate for the missing contributions from the higher levels. That is why we would like to demonstrate the results of the fit when only the data points of the first resonance region are included. We note that in [19,29] two fits to the data were also presented: the fit to the full data set (71 data points) and the fit to the region of the first resonance (32 data points). New fits to 70 data points are shown in Fig. 5 and parameters are given in Tables III and IV. We use the the logarithmic scale for the

TABLE IV. $\tilde{\chi}^2$ and $S(0)$ astrophysical factors for the $^{15}\text{N}(p, \gamma)^{16}\text{O}$ capture process obtained from the unconstrained fit $A(70)$ and constrained fit $B(70)$.

Fits	$\tilde{\chi}^2$	$S(0)$ [keVb]
Fit $A(70)$, $B_c = S_c(E_1 = 0.30872 \text{ MeV})$	1.50	37.7
Fit $B(70)$, $B_c = S_c(E_1 = 0.30872 \text{ MeV})$	1.51	37.1

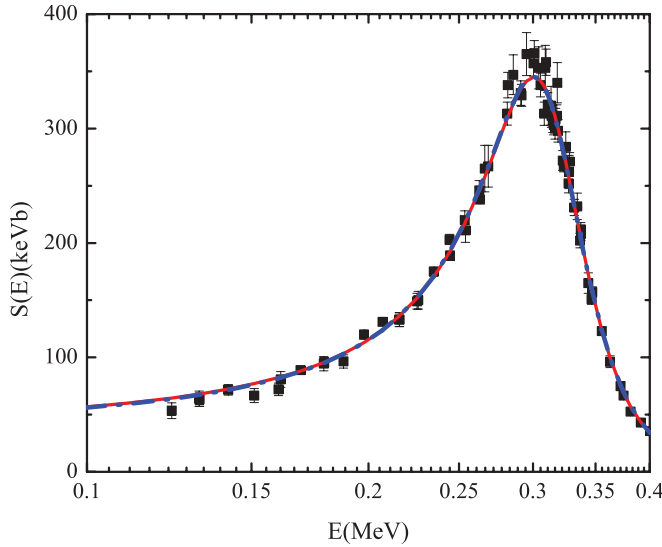


FIG. 5. (Color online) The astrophysical $S(E)$ factor for the $^{15}\text{N}(p, \gamma)^{16}\text{O}$ reaction in the low-energy region including the first resonance (70 data points). The black squares are the experimental data from Ref. [21]. The red solid line is the unconstrained fit $A(70)$ for the boundary condition $B_c = S_c(E_1 = 0.30872 \text{ MeV})$; for this fit $E_2 = 1.056 \text{ MeV}$, $\gamma_{2\gamma(\text{int})} = 0.056 \text{ MeVfm}^{3/2}$, $\gamma_{2\gamma(\text{ext})} = 0.0607 + i 0.000059 \text{ MeVfm}^{3/2}$. The blue dot-dashed line is the constrained fit $B(70)$ with the boundary condition $B_c = S_c(E_1 = 0.30872 \text{ MeV})$; for this fit $E_2 = 1.05 \text{ MeV}$, $\gamma_{2\gamma(\text{int})} = 0.082 \text{ MeVfm}^{3/2}$, $\gamma_{2\gamma(\text{ext})} = 0.052 + i 0.000051 \text{ MeVfm}^{3/2}$. The ANC is $C = 14.154 \text{ fm}^{-1/2}$.

energy axis and linear scale for the $S(E)$ factor to see more clearly the low-energy behavior of the astrophysical factors.

It is worth mentioning that both fits to 70 data points favor a lower value of the $S(0)$ factors, i.e., the same tendency which we have observed for the corresponding fits to 113 data points. The parameters of both fits are similar to the ones of the fits for 113 data points and the $S(0)$ factors are in the interval determined from the full data set fits.

V. ASTROPHYSICAL FACTORS

In Table V we present $\tilde{\chi}^2$ and $S(0)$ astrophysical factors for all our fits to 113 data points and the fit from [21].

TABLE V. $\tilde{\chi}^2$ and $S(0)$ astrophysical factors for the $^{15}\text{N}(p, \gamma)^{16}\text{O}$ capture process obtained from our fits and from the fit in [21].

Fits	$\tilde{\chi}^2$	$S(0)$ [keVb]
Ref. [21]	1.80	39.6 ± 2.6
Fit $A(113)$, $B_c = S_c(E_2)$	1.84	39.0 ± 1.1
Fit $A(113)$, $B_c = S_c(E_1)$	1.76	37.2 ± 1.0
Fit $B(113)$, $B_c = S_c(E_2)$	1.93	38.8 ± 1.1
Fit $B(113)$, $B_c = S_c(E_1)$	1.74	37.2 ± 1.0
Fit without background resonance $B_c = S_c(E_2)$	2.58	34.1 ± 1.0
Fit without background resonance $B_c = S_c(E_1)$	2.45	34.6 ± 1.0

The uncertainties of our $S(0)$ factors are obtained by a fitting to the upper (lower) border of the data obtained by adding (subtracting) the experimental uncertainties to the experimental astrophysical factor at each point. A similar procedure has been used to determine the band shown in Fig. 4.

As we can see from Table V five different fits result in quite stable $S(0)$ factors ranging in the interval $33.1 \leq S(0) \leq 40.1 \text{ keVb}$. The unconstrained fit $A(113)$ and constrained fit $B(113)$ with $B_c = S_c(E_1)$ give the minimum $\tilde{\chi}^2$ among all our fits with $S(0) = 37.2 \pm 1.0 \text{ keVb}$, which overlaps with the result reported in [21]. However, as we have discussed, the constrained fits $B(113)$ yield fitting parameters including a correct ANC value, which are more consistent with the previous estimations. In any case, our both best fits better reproduce the low-energy slope of the $S(E)$ astrophysical factor than the unconstrained fit $A(113)$ with $B_c = S_c(E_2)$, see Fig. 4, and the fit of [21], which tend away from the low-energy data, and a lower value of the $S(0)$ will be quite plausible when lower energy data become available. We also included into the list of the fits two fits performed without a background resonance, because their $\tilde{\chi}^2$ deviate from the minimum $\tilde{\chi}^2$ by < 1 . These fits provide the lowest $S(0)$ better reproducing the low-energy behavior of the $S(E)$ factor than the ones with higher $S(0)$.

VI. SUMMARY

Determination of the $S(0)$ factor for the $^{15}\text{N}(p, \gamma)^{16}\text{O}$ radiative capture is one of the goal of our fits. Although the new measurements of this reaction [21] are a real success and a very important contribution to the study of this reaction, we believe that it would be difficult to give a more accurate $S(0)$ value than the range $33.1 \leq S(0) \leq 40.1 \text{ keVb}$ determined from our fits without further measurements down to lower energies than those achieved in [21]. To get more accurate uncertainties of the $S(0)$ factor a better estimate of energy uncertainties would be also useful. From our fits we determine the interval of the astrophysical factors at the effective energy $E = 23.44 \text{ keV}$, $36.0 \text{ keVb} \leq S(E = 23.44 \text{ keV}) \leq 44.46 \text{ keVb}$. Assuming the astrophysical factor $84.1 \pm 5.9 \text{ MeVb}$ for the competing reaction $^{15}\text{N}(p, \alpha)^{12}\text{C}$ [29] we find that for every 2080_{-330}^{+410} cycles of the main CN cycle one CN catalyst is lost due to the $^{15}\text{N}(p, \gamma)^{16}\text{O}$ reaction.

But what is even more important is the question of whether the minimum of $\tilde{\chi}^2$ is always an acceptable fit. Definitely, the answer is “yes” if our knowledge about the reaction model is complete. But it is assumed that the best fit is achieved under constrained variations of the fitting parameters within the accepted boundaries obtained from the available physical information. This question elevates when the input physics is not complete. It is another goal of our analysis to demonstrate that, due to our incomplete knowledge of the reaction model, it is not canonical that a fit, which provides minimum of $\tilde{\chi}^2$, is the best from the point of view of physics. We have demonstrated here that it is possible to achieve the same or an even better fit and similar final $S(0)$ factors as in [21] by adopting the ANC measured from the transfer reaction rather than using an unconstrained variation of the ANC. But, even if the ANC

is fixed within the experimental boundaries, the question remains about the interpretation of other fitting parameters. We have demonstrated problems with the interpretation of the parameters of the fits A and the fit in [21]. Trying to improve the interpretation we fixed some parameters, which are available from the analysis of the $^{15}\text{N}(p, \alpha)^{12}\text{C}$ reaction, and we are able to achieve even better fit than in [21] and better agreement of the fitting parameters with the previous measurements of the $^{15}\text{N}(p, \gamma)^{16}\text{O}$, $^{15}\text{N}(p, \alpha)^{12}\text{C}$, $^{15}\text{N}(p, p)^{15}\text{N}$ processes and $^{12}\text{C} + \alpha$ resonance scattering [32]. However still, even our constrained fits are not fully satisfactory because we got a too high value of the radiative width of the second

resonance or a too high value of $\gamma_{2\alpha}^2$. This issue remains to be resolved.

ACKNOWLEDGMENTS

A.M.M. thanks V. Z. Goldberg and J. Millener for useful discussions. The work was supported by the US Department of Energy under Grant No. DE-FG02-93ER40773 and NSF under Grant No. PHY-0852653. M.L. acknowledges the support by the Italian Ministry of University and Research under Grant No. RBFR082838 (FIRB2008).

-
- [1] A. M. Mukhamedzhanov and N. K. Timofeyuk, Pis'ma Zh. Eksp. Teor. Fiz. **51**, 247 (1990) [JETP Lett. **51**, 282 (1990)].
- [2] A. M. Mukhamedzhanov and N. K. Timofeyuk, Sov. J. Nucl. Phys. **51**, 431 (1990).
- [3] L. D. Blokhintsev, I. Borbely, and E. I. Dolinskii, Fiz. Elem. Chastits At. Yadra **8**, 1189 (1977) [Sov. J. Part. Nuclei **8**, 485 (1977)].
- [4] E. I. Dolinsky and A. M. Mukhamedzhanov, Izv. Akad. Nauk SSSR, Ser. Fiz. **41**, 2055 (1977) [Bull. Acad. Sci. USSR, Phys. Ser. **41**, 55 (1977)].
- [5] A. M. Mukhamedzhanov and R. E. Tribble, Phys. Rev. C **59**, 3418 (1999).
- [6] A. M. Mukhamedzhanov and A. S. Kadyrov, Phys. Rev. C **82**, 051601(R) (2010).
- [7] A. M. Mukhamedzhanov, R. P. Schmitt, R. E. Tribble, A. Sattarov, Phys. Rev. C **52**, 3483 (1995).
- [8] Xiaodong Tang *et al.*, Phys. Rev. C **67**, 015804 (2003).
- [9] A. M. Mukhamedzhanov *et al.*, Phys. Rev. C **67**, 065804 (2003).
- [10] A. M. Mukhamedzhanov *et al.*, Phys. Rev. C **73**, 035806 (2006).
- [11] A. Banu *et al.*, Phys. Rev. C **79**, 025805 (2009).
- [12] T. Al-Abdullah *et al.*, Phys. Rev. C **81**, 035802 (2010).
- [13] A. M. Mukhamedzhanov *et al.*, Phys. Rev. C **78**, 015804 (2008).
- [14] Kenneth M. Nollett and R. B. Wiringa, arXiv:1102.1787 [nucl-th] (2011).
- [15] A. M. Lane and R. G. Thomas, Rev. Mod. Phys. **30**, 257 (1958).
- [16] E. G. Adelberger *et al.*, arXiv:1004.2318 (accepted for publication in Rev. Mod. Phys).
- [17] C. Rolfs and W. S. Rodney, Nucl. Phys. A **235**, 450 (1974).
- [18] D. F. Hebbard, Nucl. Phys. **15**, 289 (1960).
- [19] F. C. Barker, Phys. Rev. C **78**, 044611 (2008).
- [20] D. Bemmerer *et al.*, J. Phys. G **36**, 045202 (2009).
- [21] P. J. LeBlanc *et al.*, Phys. Rev. C **82**, 055804 (2010).
- [22] R. E. Azuma *et al.*, Phys. Rev. C **81**, 045805 (2010).
- [23] M. B. Leuschner *et al.*, Phys. Rev. C **49**, 955 (1994).
- [24] G. J. Kramer, H. P. Blokb, and L. Lapikás, Nucl. Phys. A **679**, 267 (2001).
- [25] J. C. Hiebert, E. Newman, and R. H. Bassel, Phys. Rev. **154**, 898 (1967).
- [26] W. J. W. Geurts, K. Allaart, W. H. Dickhoff, H. Muther, Phys. Rev. C **53**, 2207 (1996).
- [27] Ø. Jensen, G. Hagen, T. Papenbrock, D. J. Dean, J. S. Vaagen, Phys. Rev. C **82**, 014310 (2010).
- [28] F. C. Barker and T. Kajino, Aust. J. Phys. **44**, 369 (1991).
- [29] M. La Cognata, V. Z. Goldberg, A. M. Mukhamedzhanov, C. Spitaleri, R. E. Tribble Phys. Rev. C **80**, 012801(R) (2009).
- [30] F. C. Barker, Aust. J. Phys. **25**, 341 (1972).
- [31] F. C. Barker, Phys. Rev. C **78**, 044612 (2008).
- [32] D. R. Tilley, H. R. Weller, and C. M. Cheves, Nucl. Phys. A **565**, 1 (1993).
- [33] A. Redder *et al.*, Z. Phys. A **305**, 325 (1982).